J Clust Sci (2013) 24:273–287
DOI 10.1007/s10876-013-0550-y

ORIGINAL PAPER

Electronic and Structural Properties of Neutral, Anionic, and Cationic Rh_xCu_{4-x} ($x = 0$–4) Small Clusters: A DFT Study

A. Arab · F. Gobal · N. Nahali · M. Nahali

Received: 16 November 2012 / Published online: 9 January 2013

Abstract In this study, electronic structure, stability, and tendency to exchange electron of neutral, anionic, and cationic Rh_xCu_{4-x} ($x = 0$–4) small clusters were investigated by density functional theory calculations. For neutral small clusters, it was found that the most stable structures of Rh_4, Rh_3Cu and Rh_2Cu_2 have distorted tetrahedral shape while the most stable structures of $RhCu_3$ and Cu_4 have quasi-planer shape. Adding charges to the clusters, caused shapes of the most stable structures undergo variations. Stabilities of the neutral, anionic, and cationic clusters decrease linearly with increasing the copper content. In addition, calculated chemical harnesses indicated that the small cluster with 75 % copper content has the least chemical hardness. Interestingly, prevailing number of electronegative (Rh) and electropositive (Cu) atoms in the anionic and cationic clusters coincides with high dipole moment in these species that occur at 25 and 75 % copper respectively.

Keywords Cluster · Rh–Cu · Stability · Hardness · DFT

Electronic supplementary material The online version of this article (doi:10.1007/s10876-013-0550-y) contains supplementary material, which is available to authorized users.

A. Arab
Department of Chemistry, Semnan University, Semnan, Iran

F. Gobal
Department of Chemistry, Sharif University of Technology, Tehran, Iran

N. Nahali
Department of Physics, Shahid Beheshti University, Tehran, Iran

M. Nahali (✉)
Department of Science, Babol University of Technology, Babol, Iran
e-mail: masoud.nahali@gmail.com; masoud@nit.ac.ir

Introduction

The study of transition metal small clusters can provide insight into the fundamental changes involved in the transition from atomic to bulk structures [1]. The physical and chemical properties of the clusters are also largely determined by their size and shapes and have been the subject of both experimental and theoretical investigations [2]. Although advances have been made in experimental chemistry and physics to produce measurable quantities of size-selected clusters either in free form or on supports, the abilities to directly explore and assign cluster geometries and discriminate between possible isomers are lagging behind. Theoretical and computational studies, mainly based on density functional theory (DFT) methodologies represent the realistic way to determine electronic structures, geometries, and energies of small metallic clusters and perhaps filling the gaps. Direct calculations on small clusters and minimization of their total energy with respect to all the atomic positions have been made feasible [2–5]. The investigation of the properties of small clusters is also of fundamental importance due to their applications in surface nano structuring [6]. For example, small clusters of Pt, Rh, and Pd are used in automotive exhaust systems to reduce toxic pollutants such as CO, NO, and hydrocarbons [7].

Studies of small clusters by DFT methods have received a good deal of attentions in the past decade because of their unique catalytic properties [8–11]. Much attention has been paid to theoretical study of monometallic small clusters while bimetallic small clusters and their application in catalytic reactions are less theoretically studied [12]. Usually the catalytic activities of bimetallic surfaces are higher than monometallic surfaces because of both structural (ensemble) and electronic (ligand) effects [12, 13].

Small Rh clusters are unusual in that they are magnetic, even though bulk rhodium is nonmagnetic [14, 15]. Several groups have performed calculations to determine the structure, binding energies and magnetic properties of small Rh clusters using DFT as well as other quantum chemical techniques [16–19]. Rh appears to be an efficient catalyst for NO reduction [20] and DFT calculations have shown that NO bonds more strongly on to Rh clusters than on to Rh(1 0 0) and Rh (1 1 1), suggesting that Rh clusters may be good catalyst for NO reduction [21].

Investigation of structures and properties of copper clusters is also an attractive subject because copper and some copper alloys are highly active in various catalytic processes including hydrogenation [22, 23] and selective reduction of nitrogen oxides [24]. Copper and copper alloys clusters have also been widely used to model the Cu surface and its reactivity against atomic or molecular species [25–28]. No-pair ferromagnetic bonding in high-spin $Cu_n\,(n = 2 - 14)$ clusters have been investigated by DFT [29] and the results showed that the bond dissociation energy per atom increase to 18–19 kcal mol^{-1} with increasing the cluster size. Similar studies have been performed on $M_n\,(M = \mathrm{Cu, Ag, Au})$ clusters [30]. The valance bond analyses showed that this no-pair ferromagnetic bonding arises from bound triplet electron pairs that spread over all the close neighbors of a given atom in the clusters and causes a weak interaction in the dimer become a strong binding force that holds together monovalent atoms without a single electron pair. Tetrahedral Cu_4 cluster has been investigated by coupled-cluster method [31] and it was shown

that this structure like alkali metals clusters presents a bound quintet state and is indeed a local minimum on the potential energy surface of this system.

In the present study we employed B3PW91 DFT method to investigate the structures and energetics of neutral, anionic, and cationic Rh_xCu_{4-x} ($x = 0$–4) small clusters. Also, the stability and the tendency to exchange electron of the clusters were explained on the basis of the calculated parameters such as binding energy (BE), ionization potential (IP), electron affinity (EA), and chemical hardness.

Computational Methods

All calculations including optimization of structures, charge distributions, and vibrational frequencies of the clusters were done by the Firefly quantum chemistry software [32]. The B3PW91 hybrid density functional method has been used in this study. Commonly, a generalized gradient method such as B3PW91 is expected to give a better description of ground state properties and atomization energies than local spin density approximation (LSDA) [33]. B3PW91 hybrid functional exploits a combination of B3 exchange functional [34] and PW91 correlation functional [33, 35]. In addition, we have improved the accuracy of the calculations using modified LANL2DZ basis set. There is ample evidence in the literature that prompts us to use this method. Balbuena et al. [36] has used B3PW91 functional to study optimized geometries, electronic structures, HOMO–LUMO gaps, spin density distributions, and ionization potentials of different Cu clusters. The electronic structure of Cu_n and Al_n clusters and their interactions with atomic oxygen investigated by B3PW91 functional too [37]. Recently, B3PW91 functional has been used in the study of adsorption and dissociation of H_2O_2 on Pt and Pt-alloys small clusters [38]. Furthermore, German and Sheintuch used B3PW91 functional for study of adsorption and desorption kinetic of CO on transition metal surfaces such as Pt, Pd, Rh, Ru and Ir [39]. The Nature of the interactions between Pt_4 cluster and the adsorbates H, OH and H_2O were also investigated by DFT through B3PW91, B3LYP and BP86 functionals [40]. The natural bond orbital (NBO) charges and the corresponding dipole moments of small clusters were calculated by NBO 5.0 program [41].

Results and Discussion

In order to validate the selected method and the basis set we calculate ionization energies (IE), dissociation energies (D^0_{298}), equilibrium bond lengths and vibrational frequencies for simple Cu and Rh species. Table 1 compares the results with the available experimental data and other computed values reported in the literature. It should be noted that the values of dissociation energies were calculated by considering zero point energy and thermal corrections. Our calculated IEs of atomic Cu and Rh are 741.7 and 727.1 kJ mol^{-1} respectively, which are in agreement with the corresponding experimental values of 745.22, and 719.42 kJ mol^{-1} [42]. Also,

Table 1 Ionization energies, IEs, dissociation energies, D^0_{298}, equilibrium bond lengths, R, and vibrational frequencies of simple Cu and Rh species calculated at B3PW91 level of theory and compared with available experimental data as well as other theoretical results

Substance	IE (kJ mol^{-1})	D^0_{298} (kJ mol^{-1})	*R* (Å)	Vibrational frequency (cm^{-1})
$[Cu]^+$	741.7[a]	–	–	–
	745.22[b]			
$[Cu_2]$	–	176.1[a]	2.25[a]	260.1[a]
		201[b]	2.25[c]	256.1[i]
			2.22[h]	266.43[j]
$[Cu_2]^+$	734.9[a]	–	2.42[a]	188.9[a]
$[Rh]^+$	727.1[a]	–	–	–
	719.42[b]			
$[Rh_2]$	–	190.6[a]	2.30[a]	302.9[a]
		235.85[b]	2.21[d]	273.6[e]
			2.34[e]	267[f]
			2.28[f]	
$[Rh_2]^+$	707.8[a]		2.36[a]	270.6[a]
	700.2[e]			
	719.5[g]			

[a] This work

[b] Experimental (Ref. [42])

[c] Ref. [11]

[d] Ref. [47]

[e] Ref. [44]

[f] Experimental (Ref. [46])

[g] Experimental (Ref. [43])

[h] Experimental (Ref. [45])

[i] Ref. [12]

[j] Experimental (Ref. [48])

our calculated IE of Rh_2 is 707.8 kJ mol^{-1} which is in agreement with the experimental value of 719.5 kJ mol^{-1} [43] and the theoretically calculated value of 700.2 kJ mol^{-1} based on PW91 functional and double numerical basis set augmented with *d*-polarization and *p*-polarization functions [44]. As shown in Table 1 our calculated dissociation energies for Cu_2 and Rh_2 are 176.1 and 190.6 kJ mol^{-1} respectively. While the calculated dissociation energy of Cu_2 is in agreement with the experimental value of 201 kJ mol^{-1} [42] the calculated dissociation energy of Rh_2 is somewhat lower than the corresponding experimental value of 235.85 kJ mol^{-1} [42]. Our calculated value of 2.25 Å for equilibrium bond length of Cu–Cu is in agreement with the experimental value of 2.22 Å [45] and theoretically calculated value of 2.25 Å based on B3LYP functional and Stuttgart pseudopotential with the corresponding basis set[11]. Also, our calculated value of 2.30 Å for equilibrium bond length of Rh–Rh is in agreement with the experimental

value of 2.28 Å [46] and other theoretically calculated values of 2.21 Å based on PW91 functional using pseudopotentials and a plan wave basis set [47]. Furthermore, our calculated vibrational frequency for Rh_2 is 302.9 cm^{-1} which also is in agreement with the experimental value of 267 cm^{-1} [46] and theoretically calculated value of 273.6 cm^{-1} [44], (Table 1). Also, as shown in Table 1 our calculated vibrational frequency for Cu_2 is 260.1 cm^{-1} which is in agreement with the experimental value of 266.43 cm^{-1} [48] and theoretically calculated value of 256.1 cm^{-1} based on B3LYP functional using LANL2DZ basis set [12]. Therefore, this indicates that the selected method and the basis set are likely capable of predicting the properties of somewhat larger cluster containing Cu and Rh.

Structure and Energetic of Rh_xCu_{4-x} ($x = 0$–4) Small Clusters

The structures of neutral, anionic, and cationic Rh_xCu_{4-x} ($x = 0$–4) small clusters were optimized by B3PW91 level of theory using modified LANL2DZ basis set. All calculations involve the determination of vibrational frequencies for the validation of the local energy minima of each optimized structure. The structures with imaginary frequency(ies) are not stable [49] and have been discarded. In order to find the most stable structure of Rh_xCu_{4-x} ($x = 0$–4) clusters we calculated the total energy of each cluster, initiating with planer and tetrahedral structures, at three different spin multiplicities, $m = 1$, 3, and 5 for neutral and $m = 2$, 4, and 6 for anionic and cationic small clusters. Upon extending the calculations to higher spin multiplicities ($m = 3$, 4, 5, 6) some of the clusters are found to retain the structures attained at lower spin multiplicities ($m = 1$, 2). However, some clusters change structures while changing spin multiplicity. The structures of most stable neutral, anionic and cationic clusters are presented in Fig. 1 where distorted tetrahedral, boat and quasi-planer shapes are observed for different compositions. In this figure and other parts of this study, the letters T, B, and P behind the small cluster formula present the distorted tetrahedral, boat and quasi-planer structures, respectively. The equilibrium bond distances (in Å) are also presented on the structure of each small cluster. Increasing the copper contents of neutral, anionic, and cationic clusters tends to decrease the average bond distances of Rh–Rh, Rh–Cu, and Cu–Cu. This observation can be attributed to the shorter atomic radius of copper compared to rhodium atom.

Table 2 presents the calculated values of relative energies, binding energies (BEs), NBO charges, and Dipole moments of optimized neutral small clusters. The structures with total energy in excess of 1 eV compared to the most stable structures and the structures with imaginary frequency(ies) are discarded and therefore not shown in Table 2. The relative energies are calculated by subtracting the energy of the most stable structure from the energy of a structure in the series. For Rh_4 small cluster we found that, the most stable structure has distorted tetrahedral shape and spin multiplicity of one which is in good agreement with the literature [50] and with spin multiplicity of three the distorted tetrahedral structure is 0.13 eV less stable. Therefore, for Rh_4 clusters the optimized structures is only tetrahedrally shaped, and quasi-planer structures are unstable because of energies in excess of 1 eV compared to the most stable structure. For Rh_3Cu cluster the distorted tetrahedral shape with a

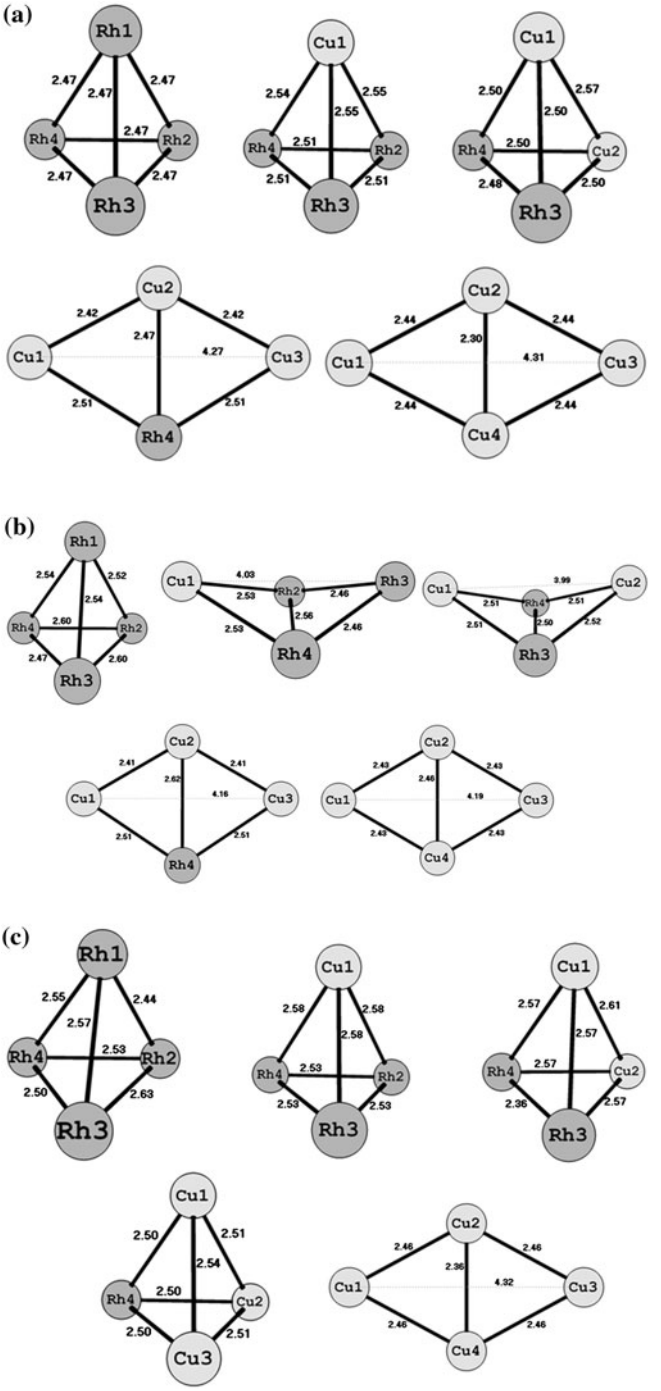

Fig. 1 Optimized structures for the most stable of **a** neutral, **b** anionic, and **c** cationic Rh_xCu_{4-x} ($x = 0$–4) small clusters

Table 2 Relative energies, BEs, NBO charges, and dipole moments of the neutral small clusters calculated at B3PW91 level of theory

Neutral cluster	Relative energy (eV)	BE (eV)	NBO charges				Dipole moments (Debye)
			1	2	3	4	
$Rh_4(m1)T^*$	0.00	**−6.85**	0.000	0.000	0.000	0.000	**0.014**
$Rh_4(m3)T$	0.13	−6.72	−0.029	−0.015	0.004	0.040	0.114
$Rh_3Cu(m3)T$	0.26	−6.45	0.213^{Cu}	−0.069	−0.071	−0.073	0.382
$Rh_3Cu(m5)T^*$	0.00	**−6.71**	0.212^{Cu}	−0.070	−0.070	−0.072	**0.603**
$Rh_2Cu_2(m1)T$	0.76	−5.51	0.198^{Cu}	0.197^{Cu}	−0.198	−0.197	1.024
$Rh_2Cu_2(m3)P$	0.66	−5.61	0.048^{Cu}	0.152^{Cu}	−0.174	−0.026	1.087
$Rh_2Cu_2(m3)T^*$	0.00	**−6.27**	0.173^{Cu}	0.173^{Cu}	−0.173	−0.173	**0.851**
$Rh_2Cu_2(m5)B$	0.51	−5.76	0.067^{Cu}	0.040^{Cu}	−0.021	−0.086	0.639
$RhCu_3(m1)P$	0.56	−5.20	0.196	−0.046	0.196	-0.346^{Rh}	0.280
$RhCu_3(m1)T$	0.18	−5.58	0.143	0.143	0.143	-0.429^{Rh}	1.480
$RhCu_3(m3)P^*$	0.00	**−5.76**	0.059	0.018	0.060	-0.138^{Rh}	**0.363**
$Cu_4(m1)P^*$	0.00	**−5.29**	−0.046	0.046	−0.046	0.046	**0.002**

* The most stable structure of each small cluster

spin multiplicity of five is the most stable structure while similar to Rh_4 cluster the quasi-planer and boat shapes are unstable and not observed. Moreover, for Rh_3Cu clusters the structures with spin multiplicity of one are not stable. For Rh_2Cu_2 clusters, the most stable structure also has a distorted tetrahedral shape and spin multiplicitiy of three while both quasi-planer and boat shapes are also stable. For $RhCu_3$ clusters on the other hand, the most stable structure has quasi-planer shape and spin multiplicity of three while the distorted tetrahedral shape having spin multiplicity of one is only 0.18 eV less stable compared to the most stable structure. For Cu_4 clusters, we found that only qausi-planer structure with spin multiplicity of one is stable which is in agreement with the literature [12, 51] and other structures were highly unstable. Therefore, it seems that with increasing the copper content of clusters the shape of the most stable structures change from distorted tetrahedral to quasi-planer structure. Moreover, the most stable structures of Rh–Cu clusters exist at higher spin multiplicities (3 or 5) compared to Rh_4 and Cu_4 clusters where most stable structures have the spin multiplicities of one.

The NBO charges in the neutral, anionic, and cationic clusters were derived by the natural population analysis (NPA). The results for neutral clusters presented on the fourth column of Table 2. NPA developed by Reed, Weinstock, and Weinhold [52] is an alternative to conventional Mulliken population analysis (MPA) and better describe the electron distribution in compounds of high ionic character. It has been reported that MPA is sensitive to basis set and may generate meaningless values whereas a distinguished feature of NPA is its independency from the basis set [53]. As can be seen in Table 2, Rh atoms that are more electronegative than Cu atoms attain negative charges and Cu atoms are usually positively charged.

Tables 3 and 4 present the calculated values of relative energies, BEs, NBO charges, and dipole moments of the anionic and cationic clusters, respectively. For

$[Rh_4]^-$ cluster (Table 3) the most stable structure has distorted tetrahedral shape and spin multiplicity of four while the structure having spin multiplicity of two which has also distorted tetrahedral shape is only 0.05 eV less stable. For $[Rh_3Cu]^-$ the structures with distorted tetrahedral and boat shapes are stable at the spin multiplicities of 2, 4, and 6 while the most stable structure has boat shape and spin multiplicity of six. For $[Rh_2Cu_2]^-$ the most stable structure has boat shape and spin multiplicity of four while the structures with distorted tetrahedral shapes are stable too. The single point calculations on negatively charged neutral Rh_2Cu_2(m3)T cluster indicate that the charge of each copper atom is 0.157 and the charge of Rh atoms are −0.672 and −0.641 while the charge of each copper atom in optimized anionic $[Rh_2Cu_2(m4)]^-B$ is −0.089 and charges of Rh atoms are −0.411 and −0.412. It seems that the high value of charge (0.157) on copper atoms in distorted tetrahedral structure causes repulsion of copper atoms and the optimized structure attain boat shape where the distance between copper atoms increases from 2.57 to 3.99 Å (Fig. 1) and repulsion between them become minimal. Similar behavior was also observed for other clusters and the optimized structures show more uniform charge distributions. Therefore, it seems that the non-uniform charge distribution forces some clusters to reconstruct and attain boat shape in order to minimize the repulsion between the atoms with same sign charges. For $[RhCu_3]^-$ and $[Cu_4]^-$ on the other hand, the most stable structures have quasi-planer shapes with spin multiplicities of four and two, respectively. For $[Cu_4]^-$, this accords with the literature [54]. Similar to the neutral

Table 3 Relative energies, BEs, NBO charges, and dipole moments of the anionic small clusters calculated at B3PW91 level of theory

Anionic cluster	Relative energy (eV)	BE (eV)	NBO charges				Dipole moments (Debye)
			1	2	3	4	
$[Rh_4(m2)]^-T$	*0.30*	−7.11	−0.283	−0.242	−0.231	−0.244	0.156
$[Rh_4(m4)]^-P$	0.55	−6.60	−0.250	−0.250	−0.250	−0.250	0.008
$[Rh_4(m4)]^-T^*$	0.00	**−7.15**	−0.278	−0.166	−0.278	−0.278	**0.172**
$[Rh_3Cu(m2)]^-T$	*0.6*	−6.45	0.014^{Cu}	−0.338	−0.340	−0.335	0.175
$[Rh_3Cu(m4)]^-B$	*0.45*	−6.52	-0.137^{Cu}	−0.218	−0.295	−0.349	0.637
$[Rh_3Cu(m4)]^-T$	0.18	−6.76	-0.005^{Cu}	−0.339	−0.339	−0.317	0.147
$[Rh_3Cu(m6)]^-B^*$	0.00	**−6.95**	-0.118^{Cu}	−0.287	−0.308	−0.287	**0.645**
$[Rh_2Cu_2(m2)]^-T$	*0.80*	−6.18	-0.087^{Cu}	-0.142^{Cu}	−0.390	−0.380	0.362
$[Rh_2Cu_2(m4)]^-B^*$	0.00	**−6.61**	-0.089^{Cu}	-0.088^{Cu}	−0.412	−0.411	**0.408**
$[Rh_2Cu_2(m6)]^-T$	0.54	−6.07	-0.143^{Cu}	-0.145^{Cu}	−0.354	−0.358	0.266
$[RhCu_3(m2)]^-P$	0.10	−6.15	−0.233	−0.119	−0.233	-0.415^{Rh}	0.536
$[RhCu_3(m4)]^-P^*$	0.00	**−6.25**	−0.107	−0.312	−0.106	-0.475^{Rh}	**0.067**
$[RhCu_3(m4)]^-T$	0.90	−5.35	−0.169	−0.092	−0.174	-0.564^{Rh}	1.075
$[Cu_4(m2)]^-P^*$	0.00	**−5.93**	−0.168	−0.332	−0.168	−0.332	**0.001**
$[Cu_4(m2)]^-T$	0.84	−5.08	−0.277	−0.323	−0.198	−0.201	0.979
$[Cu_4(m4)]^-T$	0.57	−5.36	−0.250	−0.250	−0.250	−0.250	0.297

* The most stable structure of each small cluster

clusters with increasing the copper content of anionic clusters the shape of the most stable structures change from distorted tetrahedral to quasi-planer. The NBO charges (fourth column of Table 3) demonstrate that large part of the negative charge of small clusters accumulates on the Rh atoms.

As presented in Table 4, for the cationic clusters the quasi-planer shape is the most stable structure only for $[Cu_4]^+$ and for other clusters including $[Rh_4]^+$ and Rh/Cu clusters the most stable structures have distorted tetrahedral shape. Therefore, it seems that with increasing the copper content of cationic small clusters the shape of the most stable structures retains distorted tetrahedral. Also, for cationic small clusters the boat shape is not observed as a stable structure for none of the small clusters in contrast to the neutral and anionic small clusters (perhaps because of more uniform charge distribution in cationic small clusters which minimize the repulsion between atoms with same sign charges). The NBO charges (fourth column of Table 4) demonstrate that Cu atoms are more positively charged compared to the Rh atoms.

The values of binding energies of neutral small clusters have been calculated according to the following equation:

$$-\mathrm{BE} = E(\mathrm{Rh}_x\mathrm{Cu}_{4-x}) - xE(\mathrm{Rh}) - (4-x)E(\mathrm{Cu}), \quad x = 0-4 \tag{1}$$

where $E(\mathrm{Rh}_x\mathrm{Cu}_{4-x})$ is the total energy of neutral cluster and $E(\mathrm{Rh})$ and $E(\mathrm{Cu})$ are the total energies of Rh and Cu atoms in the most stable states, respectively.

For anionic clusters, the values of binding energies have been calculated according to the following equations [7]

Table 4 Relative energies, BEs, NBO charges, and dipole moments of the cationic small clusters calculated at B3PW91 level of theory

Cationic cluster	Relative energy (eV)	BE (eV)	NBO charges				Dipole moments (Debye)
			1	2	3	4	
$[Rh_4(m2)]^+T$	*0.20*	−7.56	0.247	0.251	0.245	0.257	0.078
$[Rh_4(m4)]^+T^*$	0.00	**−7.78**	0.218	0.249	0.272	0.261	**0.091**
$[Rh_3Cu(m2)]^+T$	0.49	−7.65	0.382^{Cu}	0.162	0.232	0.224	0.974
$[Rh_3Cu(m4)]^+T$	0.39	−7.75	0.390^{Cu}	0.204	0.203	0.203	0.945
$[Rh_3Cu(m6)]^+T^*$	0.00	**−8.14**	0.367^{Cu}	0.211	0.211	0.211	**0.873**
$[Rh_2Cu_2(m2)]^+T$	0.34	−7.42	0.346^{Cu}	0.346^{Cu}	0.154	0.154	1.699
$[Rh_2Cu_2(m4)]^+P$	0.84	−6.92	0.371^{Cu}	0.373^{Cu}	0.127	0.128	1.677
$[Rh_2Cu_2(m4)]^+T^*$	0.00	**−7.77**	0.345^{Cu}	0.345^{Cu}	0.155	0.156	**1.793**
$[RhCu_3(m2)]^+P$	0.58	−6.86	0.283	0.383	0.283	0.050^{Rh}	0.893
$[RhCu_3(m2)]^+T^*$	0.00	**−7.44**	0.310	0.307	0.310	0.073^{Rh}	**1.866**
$[Cu_4(m2)]^+P^*$	0.00	**−6.52**	0.175	0.325	0.175	0.325	**0.011**
$[Cu_4(m2)]^+T$	0.32	−6.20	0.251	0.250	0.252	0.247	0.017

* The most stable structure of each small cluster

$$-\mathrm{BE} = E(\mathrm{Rh}_x\mathrm{Cu}_{4-x})^- - (x-1)E(\mathrm{Rh}) - E(\mathrm{Rh})^- - (4-x)E(\mathrm{Cu}), \quad x = 1-4 \tag{2}$$

$$-\mathrm{BE} = E(\mathrm{Cu}_4)^- - E(\mathrm{Cu})^- - 3E(\mathrm{Cu}) \tag{3}$$

where $E(\mathrm{Rh}_x\mathrm{Cu}_{4-x})^-$ is the total energy of anionic small cluster and $E(\mathrm{Rh})^-$, $E(\mathrm{Cu})^-$ are the total energies of anionic Rh and Cu atoms in the most stable states, respectively. Since Rh is more electronegative than Cu, in Eq. (2) we assume that anionic $\mathrm{Rh}_x\mathrm{Cu}_{4-x}$ clusters are formed from one anionic Rh, $(x-1)$neutral Rh and $(4-x)$neutral Cu.

And for cationic clusters, the equations used for binding energies calculations are [7]

$$-\mathrm{BE} = E(\mathrm{Rh}_x\mathrm{Cu}_{4-x})^+ - xE(\mathrm{Rh}) - E(\mathrm{Cu})^+ - (3-x)E(\mathrm{Cu}), \quad x = 0-3 \tag{4}$$

$$-\mathrm{BE} = E(\mathrm{Rh}_4)^+ - E(\mathrm{Rh})^+ - 3E(\mathrm{Rh}) \tag{5}$$

where, $E(\mathrm{Rh}_x\mathrm{Cu}_{4-x})^+$ is the total energy of cationic cluster and $E(\mathrm{Rh})^+$, $E(\mathrm{Cu})^+$ are the total energies of cationic Rh and Cu atoms in the most stable states, respectively. Because Cu is more electropositive than Rh, in Eq. (4) we assume that cationic $\mathrm{Rh}_x\mathrm{Cu}_{4-x}$ small clusters are formed from one cationic Cu, x neutral Rh and $(3-x)$ neutral Cu.

Variation of binding energies of the most stable structures of all the small clusters (the bold values in the third columns of Tables 2, 3, and 4) as a function of copper percentage is presented in Fig. 2. It is observed that, the BE drops linearly with increasing the copper content with the correlation coefficients of 0.972 and 0.992 for neutral and anionic small clusters, respectively while for cationic clusters the mentioned dependency is far from linear behaviour. The fall of BE shows that the stabilities of neutral, anionic, and cationic small clusters decrease with increasing

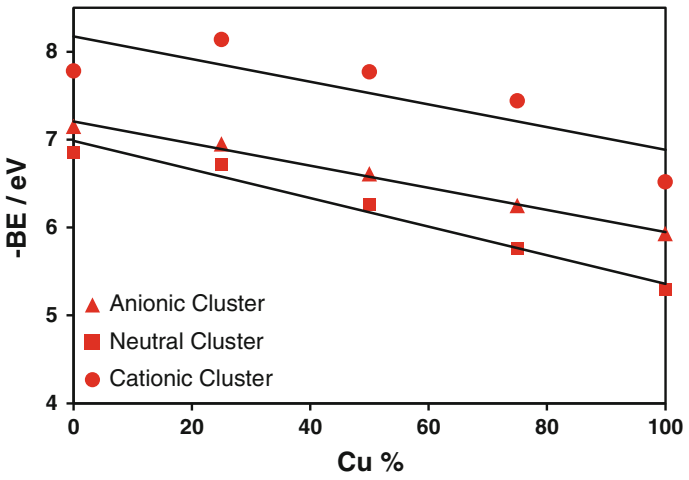

Fig. 2 The variation of binding energy of the most stable structures of all small clusters against copper percentage

the copper content. In the other word, Rh–Cu small clusters are more stable than Cu_4 small clusters and less stable than Rh_4 small clusters.

Global Hardness and Dipole Moment of Rh_xCu_{4-x} ($x = 0$–4) Small Clusters

Several reactivity descriptors are used in DFT to define the reactivity of molecules. One such descriptor is global (chemical) hardness (η), which is defined as the second derivative of energy with respect to the number of electrons at constant external potential. Using the finite difference approximation chemical hardness can be expressed as [7, 55]

$$\eta = \frac{\mathrm{IP} - \mathrm{EA}}{2} \tag{6}$$

where IP and EA are the first ionization potential and EA of the chemical system.

Chemical hardness is resistance of a chemical entity to change in the number of electrons. Energetically speaking, hardness is one-half of the energy change for the disproportionation of a special chemical species according to the following reaction [55]

$$S + S \rightarrow S^+ + S^- \tag{7}$$

Since always $\mathrm{IP_S} \geq \mathrm{EA_S}$, the minimum value of hardness is zero. Zero hardness indicates maximum softness and maximum softness means no energy change associated with the disproportionation reaction as Eq. (7). For example a bulk metal has IP = EA ($\eta = 0$) and maximum softness [55].

We have calculated the adiabatic ionization potential (AIP) and adiabatic electron affinity (AEA) using the following equations [7]:

$$\mathrm{AIP} = E_n^+ - E_n \tag{8}$$

$$\mathrm{AEA} = E_n - E_n^- \tag{9}$$

where E_n is the total energy of neutral small cluster, E_n^+ and E_n^- are the total energies of cationic and anionic small clusters at the optimized geometry of cation and anion, respectively. The variations of AIP and AEA of the most stable structures of all small clusters as a function of copper percentage are presented in Fig. 3. Variations of AIP indicate that adding copper to the Rh small cluster decreases AIP to reach a minimum at 75 % copper and being lower than the AIP of Cu small cluster (Fig. 3a). Also, adding copper to the Rh small cluster reduces AEA to reach a minimum at 25 % copper and with further increasing the copper content AEA increases to the value calculated for Cu small cluster (Fig. 3b).

Figure 4 presents the variation of the global hardness of the most stable structure of all clusters against copper percentage. As it can be seen in the figure with increasing copper content the chemical hardness decreases to a minimum at 75 % copper content. Therefore, the small cluster with 75 % copper content has the maximum softness among these small clusters. It means that $RhCu_3$ cluster has maximum tendency to exchange electrons. Moreover, it is clear from Fig. 4 that all three Rh–Cu clusters are softer than Rh_4 cluster, which means that the tendency to

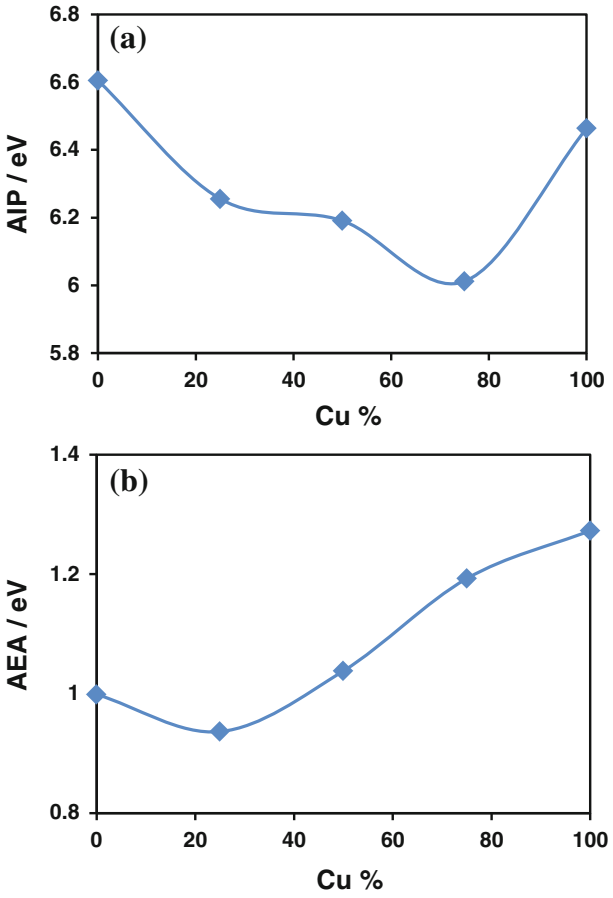

Fig. 3 The variation of AIP (**a**) and AEA (**b**) of the most stable structures of all small clusters against copper percentage

exchange electrons in the Rh–Cu small clusters is easier compared to that in the Rh_4 cluster.

Another calculated property of Rh_xCu_{4-x} ($x = 0$–4) clusters is dipole moment which are shown in the last columns of Tables 2, 3, and 4 for neutral, anionic and cationic small clusters, respectively. Figure 5 presents the variation of dipole moments of the most stable structures (the bold values presented in the last columns of Tables 2, 3 and 4) of all small clusters against copper percentage. As shown in this figure, the maximum dipole moment for anionic and cationic small clusters occurs at 25 and 75 % copper contents where the number of electronegative (Rh) and electropositive (Cu) atoms prevail respectively. Also, for the neutral clusters the maximum dipole moment occurs where the number of electropositive and electronegative atoms are equal that is in accordance with our chemistry comprehension.

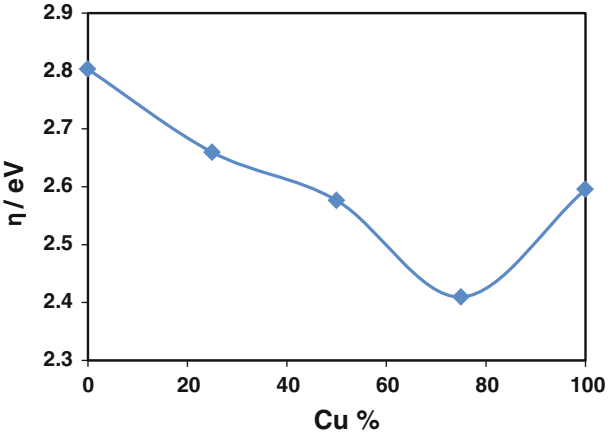

Fig. 4 The variation of the global hardness of the most stable structures of all small clusters against copper percentage

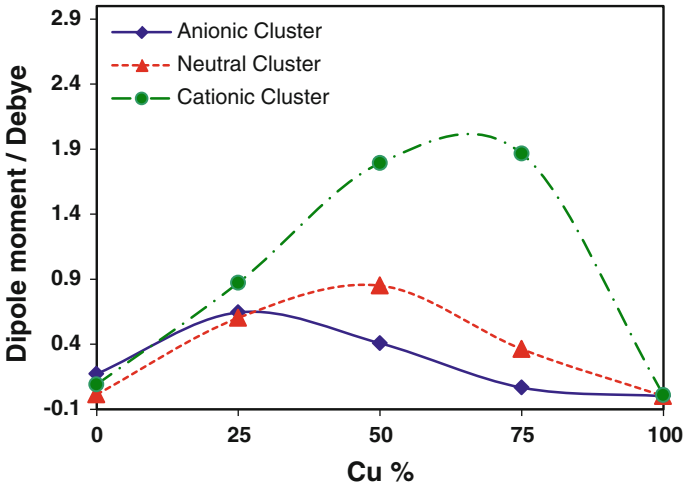

Fig. 5 The variation of dipole moment of the most stable structures of all small clusters against copper percentage

Conclusions

We have employed DFT method to study the structure, stability, and chemical hardness of neutral, anionic, and cationic Rh_xCu_{4-x} ($x = 0$–4) small clusters. Following are the main findings of this study:

(I) For neutral clusters, the most stable structures of Rh_4, Rh_3Cu and Rh_2Cu_2 have distorted tetrahedral shape with spin multiplicities of 1, 5, and 3 while the most stable structures of $RhCu_3$ and Cu_4 have quasi-planer shape with spin multiplicities of three and one, respectively.

(II) For anionic clusters, the most stable structure of $[Rh_4]^-$ has distorted tetrahedral shape with spin multiplicity of four while for $[Rh_3Cu]^-$ and $[Rh_2Cu_2]^-$ the structures with boat shape with spin multiplicities of 6, 4 and for $[RhCu_3]^-$ and $[Cu_4]^-$, structures with quasi-planer shape with spin multiplicities of four and two, respectively are the most stable structures.

(III) For cationic clusters, the most stable structures of $[Rh_4]^+$, $[Rh_3Cu]^+$, $[Rh_2Cu_2]^+$, and $[RhCu_3]^+$ have distorted tetrahedral shapes with spin multiplicities of 4, 6, 4, and 2 respectively while the most stable structure of $[Cu_4]^+$ has quasi-planer shape with spin multiplicity of two.

(IV) With increasing the copper content of neutral and anionic clusters the structure of most stable small cluster change from distorted tetrahedral to quasi-planer shape while for cationic small clusters the shape of most stable structure remain distorted tetrahedral.

(V) The non-uniform charge distribution forces some clusters to reconstruct and attain boat shape in order to minimize the repulsion between the atoms with same sign charges. Reconstruction of structure in clusters has been observed with changing of electrical charge.

(VI) Calculation of binding energies indicated that higher copper content has detrimental effect on the stability of small clusters while the calculated chemical hardness shows a minimum at 75 % copper content corresponds to the maximum softness.

(VII) The maximum dipole moment for anionic and cationic small clusters occurs at 25 and 75 % copper contents where the number of electronegative (Rh) and electropositive (Cu) atoms prevail respectively.

Acknowledgments The authors gratefully acknowledge the Office of the Vice Chancellor of Research of Sharif University of Technology, Babol Noshirvani University of Technology, and Semnan University for financial supports of this work.

References

1. D. J. Harding, T. R. Walsh, S. M. Hamilton, W. S. Hopkins, S. R. Mackenzie, P. Gruene, M. Haertelt, G. Meijer, and A. Fielicke (2010). *J. Chem. Phys.* **132**, 011101.
2. J. L. Rao, G. K. Chaitanya, S. Basavaraja, K. Bhanuprakash, and A. Venkataramana (2007). *J. Mol. Struct. THEOCHEM* **803**, 89.
3. M. Nahali and F. Gobal (2010). *Mol. Phys.* **108**, 1317.
4. M. Nahali and F. Gobal (2009). *Mol. Phys.* **107**, 1805.
5. J. Scaranto and S. Giorgianni (2009). *Mol. Phys.* **107**, 1997.
6. M. Karabacak, S. Ozcelik, and Z. B. Guvenc (2003). *Surf. Sci.* **532–535**, 306.
7. B. Kalita and R. C. Deka (2007). *J. Chem. Phys.* **127**, 244306.
8. G. Lv, F. Wei, H. Jiang, Y. Zhou, and X. Wang (2009). *J. Mol. Struct. THEOCHEM* **915**, 98.
9. F. Gobal, R. Arab, and M. Nahali (2010). *J. Mol. Struct. THEOCHEM* **959**, 15.
10. A. Pundt, M. Suleiman, C. Bahtz, M. T. Reetz, R. Kirchheim, and N. M. Jisrawi (2004), *Mater. Sci. Eng. B* **108**, 19.
11. L. P. Campos (2007). *J. Mol. Struct. THEOCHEM* **815**, 63.
12. I. Efremenko and M. Sheintuch (2005). *Chem. Phys. Lett.* **401**, 232.
13. S. Gonzalez, C. Sousa, M. Fernandez-Garcıa, V. Bertin, and F. Illas (2002). *J. Phys. Chem. B* **106**, 7839.

14. B. V. Reddy, S. N. Khanna, and B. I. Dunlap (1993). *Phys. Rev. Lett.* **70**, 3323.
15. A. J. Cox, J. G. Louderback, and L. A. Bloomfield (1993). *Phys. Rev. Lett.* **71**, 923.
16. Y. C. Bae, H. Osanai, V. Kumar, and Y. Kawazoe (2004). *Phys. Rev. B* **70**, 195413.
17. T. Futschek, M. Marsman, and J. Hafner, (2005) *J. Phys. Condens. Matter* **17**, 5927.
18. A. Endou, N. Ohashi, K. Yoshizawa, S. Takami, M. Kubo, A. Miyamoto, and E. Broclawik (2000). *J. Phys. Chem. B* **104**, 5110.
19. D. Harding, S. R. Mackenzie, and T. R. Walsh (2006). *J. Phys. Chem. B* **110**, 18272.
20. D. Loffreda, D. Simon, and P. Sautet (1998). *J. Chem. Phys.* **108**, 6447.
21. P. Ghosh, R. Pushpa, S. D. Gironcoli, and S. Narasimhan (2008). *J. Chem. Phys.* **128**, 194708.
22. K. Sugiyama, H. Miura, Y. Watanabe, and Y. Ukai (1987). *Bull. Chem. Soc. Jpn.* **60**, 1579.
23. Y. Yang, J. Evans, J. A. Rodriguez, J. A. Rodriguez, M. G. White, and P. Liu (2010). *Phys. Chem. Chem. Phys.* **12**, 9909.
24. T. Miyadera (1998). *Appl. Catal. B* **16**, 155.
25. G. De and C. N. R. Rao (2003). *J. Phys. Chem. B* **107**, 13597.
26. J. Torras, C. L. Dufaure, N. Russo, and J. M. Ricart (2001). *J. Mol. Catal. A* **167**, 109.
27. Y. Okamoto (2005). *Chem. Phys. Lett.* **405**, 79.
28. B. Gomes, J. A. N. F. Gomes, and F. Illas (2001). *J. Mol. Catal. A* **170**, 187.
29. S. P. de Visser, D. Kumar, M. Danovich, N. Nevo, D. Danovich, P. K. Sharma, W. Wu, and S. Shaik (2006). *J. Phys. Chem. A* **110**, 8510.
30. D. Danovich and S. Shaik (2010). *J. Chem. Theory Comput.* **6**, 1479.
31. M. Verdicchio, S. Evangelisti, T. Leininger, J. Sanchez-Marin, and A. Monari (2011). *Chem. Phys. Lett.* **503**, 215.
32. A. A. Granovsky (2009). Firefly version 7.1.G. http://classic.chem.msu.su/gran/firefly/index.html.
33. J. P. Perdew, J. A. Chevary, S. H. Vosko, K. A. Jackson, M. R. Pederson, D. J. Singh, and C. Fiolhais (1992). *Phys. Rev. B.* **46**, 6671.
34. A. D. Becke (1993). *J. Chem. Phys.* **98**, 1372.
35. J. P. Perdew and Y. Wang (1992). *Phys. Rev. B* **45**, 13244.
36. P. B. Balbuena, P. A. Derosa, and J. M. Seminario (1999). *J. Phys. Chem. B* **103**, 2830.
37. C. Lacaze-Dufaure, C. Blanc, G. Mankowski, and C. Mijoule (2007). *Surf. Sci.* **601**, 1544.
38. P. B. Balbuena, S. R. Calvo, E. J. Lamas, P. F. Salazar, and J. M. Seminario (2006). *J. Phys. Chem. B* **110**, 17452.
39. E. D. German and M. Sheintuch (2008). *J. Phys. Chem. C* **112**, 14377.
40. R. L. T. Parreira, G. F. Caramori, S. E. Galembeck, and F. Huguenin (2008). *J. Phys. Chem. A* **112**, 11731.
41. E. D. Glendening, J. K. Badenhoop, A. E. Reed, J. E. Carpenter, J. A. Bohmann, C. M. Morales, and F. Weinhold *Theoretical Chemistry Institute* (University of Wisconsin, Madison, 2001).
42. D. R. Lide (ed.) *CRC Handbook of Chemistry and Physics*, 89th ed (CRC Press/Taylor and Francis, Boca Raton, 2009).
43. D. L. Cocke and K. A. Gingerich (1974). *J. Chem. Phys.* **60**, 1958.
44. J. Lv, F. Q. Zhang, X. H. Xu, and H. S. Wu (2009). *Chem. Phys.* **363**, 65.
45. K. P. Huber and G. Herzberg *Constants of Diatomic Molecules, Molecular Spectra and Molecular Structure*, vol. IV (Van Nostrand Reinhold Company, Princeton, 1979).
46. K. A. Gingerich and D. L. Cocke (1972). *J. Chem. Soc. Chem. Commun.* **1**, 536.
47. S. Dennler, J. Morillo, and G. M. Pastor (2003). *Surf. Sci.* **532–535**, 334.
48. E. A. Rohlfing and J. J. Valentini (1986). *J. Chem. Phys.* **84**, 6560.
49. V. Bertani, C. Cavallotti, M. Masi, and S. Carra (2003). *J. Mol. Catal. A Chem.* **204–205**, 771.
50. D. S. Mainardi and P. B. Balbuena (2003). *J. Phys. Chem. A* **107**, 10370.
51. V. E. Matulis and O. A. Ivaskevich (2006). *Comput. Mater. Sci.* **35**, 268.
52. A. E. Reed, R. B. Weinstock, and F. Weinhold (1985). *J. Chem. Phys.* **83**, 735.
53. A. E. Reed, L. A. Curtiss, and F. Weinhold (1988). *Chem. Rev.* **88**, 899.
54. V. E. Matulis, O. A. Ivaskevich, and V. S. Gurin (2004). *J. Mol. Struct. THEOCHEM* **681**, 169.
55. R. G. Parr and R. G. Pearson (1983). *J. Am. Chem. Soc.* **105**, 7512.